Journal of Nano Research Vols. 18-19 (2012) pp 149-155
Online available since 2012/Jul/26 at www.scientific.net

doi:10.4028/www.scientific.net/JNanoR.18-19.149

Arsenic sulphide As_4S_4 nanoparticles: Physico-chemical properties and anticancer effects

Peter Baláž[1, a], Ján Sedlák[2,b], Michal Pastorek[2,c], Danka Cholujová[2,d], Kandasamy Vignarooban[3,e], Siddhesh Bhosle[3,f], Punit Boolchand[3,g], Zdenka Bujňáková[1,h], Erika Dutková[1,i], Olga Kartachova[4,j;5,k], Bernhardt Stalder[4,l]

[1] Institute of Geotechnics, Slovak Academy of Sciences, 043 53 Košice, Slovakia

[2] Cancer Research Institute, Slovak Academy of Sciences, 833 91 Bratislava, Slovakia

[3] Department of Electrical and Computer Engineering, University of Cincinnati, Ohio 45221-0030, USA

[4] Bühler AG, 92 40 Uzwil, Switzerland

[5]Deakin University, Waurn Ponds, Australia

[a]balaz@saske.sk, [b]Jan.Sedlak@savba.sk, [c]exonpast@savba.sk, [d]exondach@savba.sk, [g]boolchp@ucmail.uc.com, [h]bujnakova@saske.sk, [i]dutkova@saske.sk, [l]bernhard.stalder@buhlergroup.com

Keywords: arsenic sulphide, nanoparticles, milling, cancer.

Abstract. In this study, arsenic sulphide As_4S_4 nanoparticles have been prepared, by high-energy wet milling, in the presence of sodium dodecylsulphate, which acts a surfactant. Solid state properties of the nanoparticles were characterised by XRD, Raman scattering, specific surface area and particle size distribution. Changes in surface areas of the particles, in the 0.2 - 5.4 $m^2 g^{-1}$ range, and nanosize distributions, in the 100 - 250 nm range, characterise the surface and morphological properties of nanorealgar. Raman scattering revealed various species in the milled sample that indicate a disproportionate reaction ($3As_4S_4 \rightarrow 4As_2S_3 + 4As$) occurring as a consequence of milling. Anticancer effects, of the milled species, were confirmed for the human multiple myeloma U266 and OPM1 cell lines. Dissolution experiments in simulated gastric fluid show a possibility for the application of the realgar nanoparticles as an oral dose in future arsenic drug cancer treatments.

Introduction

Arsenic sulphide As_4S_4 is a red semiconductor that exists in several crystalline forms. The room temperature, stable form is chemically identical to mineral realgar [1]. Realgar is a versatile substance classified as an advanced material as well as a curative agent. Recently, interesting optical properties have been described with possible applications in optoelectronic materials [2]. Particulate realgar has also been studied as a drug for cancer treatment [3, 4]; however, its solubility (and consequently bioavailability) is low, and some sort of pretreatment is needed.

Mechanochemistry, which applies several modes of high-energy milling (including nanomilling), involves the mechanical pretreatment of solids [5]. Nanomilling seems to be an effective pretreatment procedure that modifies the physico-chemical properties, as well as the solubility and bioavailability of particles [6-7]. Recently, high-energy milling has been applied to the synthesis of a wide variety of nanocrystalline materials [8-11]. The efforts in mechanochemistry, to modify the properties of nanocrystalline powders, also brought new stimuli into pharmaceutical science [12-14]. Here, the increase in dissolution velocity and the improved bioavailability plays a crucial role in the application of new drugs.

The aim of this paper is to examine the influence of nanomilling on the physico-chemical properties and dissolution of arsenic sulphide nanoparticles and their impact on the viability of several cancer cell lines.

Experimental

The investigation was carried out with arsenic sulphide As_4S_4 sample (Sigma-Aldrich, USA). The XRD performed by employing an X-ray diffractometer Miniflex (Rigaku, Japan) estimated arsenic sulphide (JCPDS 48-1247) as the only present crystalline phase.

The nanomilling has been performed in a laboratory attritor PE-075 (Netzsch, Germany) in presence of 200 ml of 0.075 % sodium dodecylsulphate solution as a surfactant. The following milling conditions were applied: material of the milling balls: yttrium stabilized ZrO_2, loading of the mill with 1176 grams of 1.5 mm diameter balls, rotation speed of the mill shaft 1000 min^{-1}, milling time 10-90 min.

The specific surface area was determined by the low temperature nitrogen adsorption method in a Gemini 2360 sorption apparatus (Micromeritics, USA).

Particle size distribution was measured on the particle size analyser Nanophox (Sympatec, Germany) based on the photon cross-correlation spectroscopy.

Raman micro-spectroscopy was studied using a dispersive T64000 triple monochromator system (Horiba-Jobin Yvon, USA) using 647 nm excitation. The dispersive system made use of a microscope attachment with an 80x objective bringing laser light to a fine focus (1 μm spot size) and the scattered radiation detected using a charge-coupled device (CCD) detector.

Simulated gastric fluid SGF (without pepsin) of composition 0.2 % sodium chloride in 0.7 % hydrochloric acid [15] has been applied at 36 °C for dissolution experiments.

Anticancer effect of arsenic sulphide particles has been tested by standard methods [16]. For biological testing human multiple myeloma cancer cell lines U266 and OPM1 have been selected. Cells were incubated in fluorescein-diacetate (10 nM) in PBS for 30 min, then chilled, co-stained with propidium iodide (10 μg/mL final concentration) and analyzed using Altra flow cytometer as published in [17].

Results and discussion

Surface changes. The disintegration of arsenic sulphide particles by high-energy milling is accompanied by an increase of their number and by the generation of fresh, previously unexposed surfaces. The dependence of the specific adsorption surface on the time of milling is presented in Fig. 1. The trace show, that the rate of new surface area formation is limited by the time of milling. After the first stage, where the increase in values of S_A is relatively sharp, the second stage is manifested at a milling time $t_M > 30$ min. Here, the slower formation of the new surface area can be detected. In this stage, the so-called “mechanochemical equilibrium” plays decisive role [5]. The smaller particles are put together to form larger entities in which the original particles can still be identified.

Nanoparticles size distribution. The size distribution of arsenic sulphide nanoparticles, given in Fig. 2, can offer a deeper look into the milling process. At the first stage of milling ($t_M \leq 30$ min), a mono-modal distribution of the particles is exhibited; the main particle populations have the average hydrodynamic parameters of 212 and 162 nm for the milling times of 10 and 30 min., respectively. At the second stage of milling ($t_M \geq 30$ min), the particles are larger and their distribution is changed from mono- to bi-modal. In addition to the small particles, larger entities are also formed with particle sizes 500 - 550 nm. Experience shows, after the achievement of a certain degree of dispersion, that further comminution is reduced or that there may even be an increase in the particle size due to the interaction of the particles [18]. This was also clearly demonstrated for our mode of nanomilling.

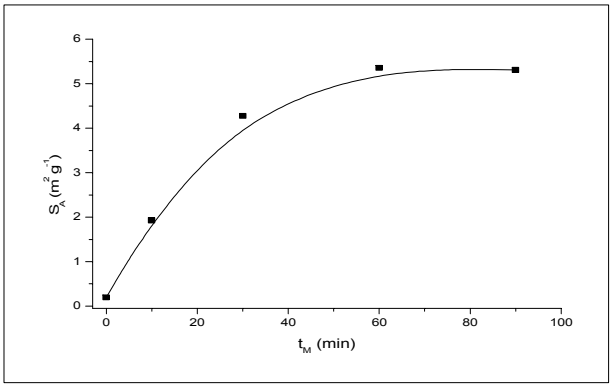

Fig. 1 Specific surface area, S_A vs. milling time, t_M of arsenic sulphide nanoparticles

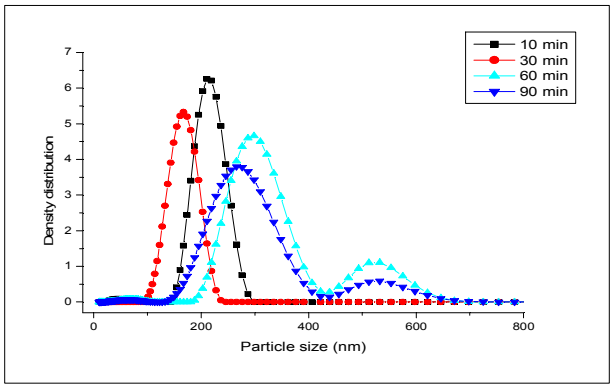

Fig. 2 Size distribution of arsenic sulphide nanoparticles

Bulk changes. The structure of the milled arsenic sulphide was elucidated using the Raman scattering method. For this test, a sample that was milled for 30 minutes was selected. To analyse the Raman lineshape of the sample, the Raman scattering of the reference samples, As_4S_4 (non-milled) and As_2S_3 (non-milled), was also recorded (Fig. 3). In all three samples, we can observe a Raman lineshape that is, more or less, common and representative of the majority phase in the samples. The line shape is extremely rich; close to 12 lines are observed, which are all reasonably well-resolved. The spectra at the top of Fig. 3 show that the dominant features of Raman plots are bands (i) in the 150 – 260 cm^{-1} region, with maxima at 185.219 and 231.4 cm^{-1}, and (ii) in the 300 – 370 cm^{-1} region, with maxima at 342.4 and 359.3 cm^{-1}. Generally, Raman frequencies at 150 – 260 cm^{-1} and 300 – 370 cm^{-1} can be assigned to As-As-S bending and As-S stretching modes of realgar, respectively [19-21]. The peak at 271.5 cm^{-1} belongs to pararealgar [22-23]. However, in comparison with the reference spectra of As_2S_3 (Fig. 3, bottom), there is also coincidence with bands at 136.4, 179.1, 202.5, 292.9 and 382.7 cm^{-1}. Moreover, the bands for amorphous elemental As (a-As) are also detected in the milled sample. Based on this fact, and the microscopic observation where an arsenic-rich product and arsenic-deficient product is observable, the milling can be crudely described by the disproportional reaction (1)

$$3As_4S_4 \xrightarrow{\text{milling}} 4As_2S_3 + 4As \qquad (1)$$

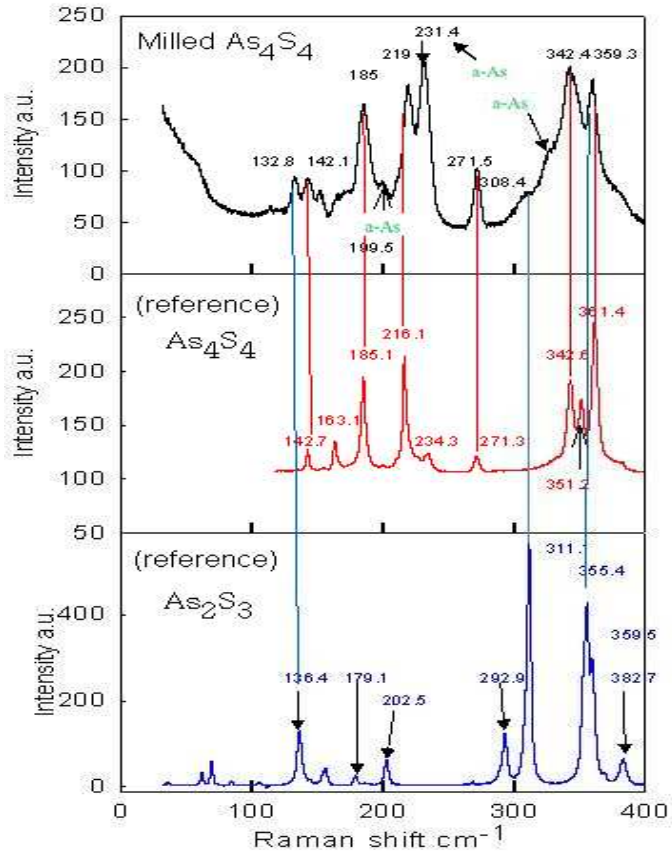

Fig. 3 Raman lineshape of arsenic sulphide nanoparticles: top - sample milled for 30 min, middle - reference As_4S_4 (non-milled), bottom - reference As_2S_3 (non-milled)

Anticancer effect. In the present study, a cytotoxic effect of the milled realgar nanoparticles is demonstrated. For the evaluation of the nanoparticles activity, two human multiple myeloma (MM) cell lines, U266 and OPM1, were selected (MM is a cancer of the plasma cell, an important part of the human immune system producing antibodies to help fight infection and disease). The results are shown in Fig. 4, which shows the dependence of the parameter IC_{50} on the specific surface area values, S_A, of the milled samples (IC_{50} represents the concentration of arsenic that is required for a 50% inhibition of the cells in comparison with the control sample). For comparison, the values of IC_{50} for arsenic oxide As_2O_3 are also included in Fig. 4. Today, arsenic oxide is accepted as an acute leukaemia treatment; however, its toxicity is high and possesses severe side effects in drug form [24]. The sensitivity on the surface area values of arsenic sulphide nanoparticles is clearly demonstrated for both cell lines. The MM cell lines OPM1 are more resistant and less sensitive to the surface properties of arsenic sulphide, in comparison with the cell lines U266. Their efficiency, however, in comparison with the IC_{50} values for As_2O_3, is clearly demonstrated. The larger the values of S_A, then a larger difference is documented.

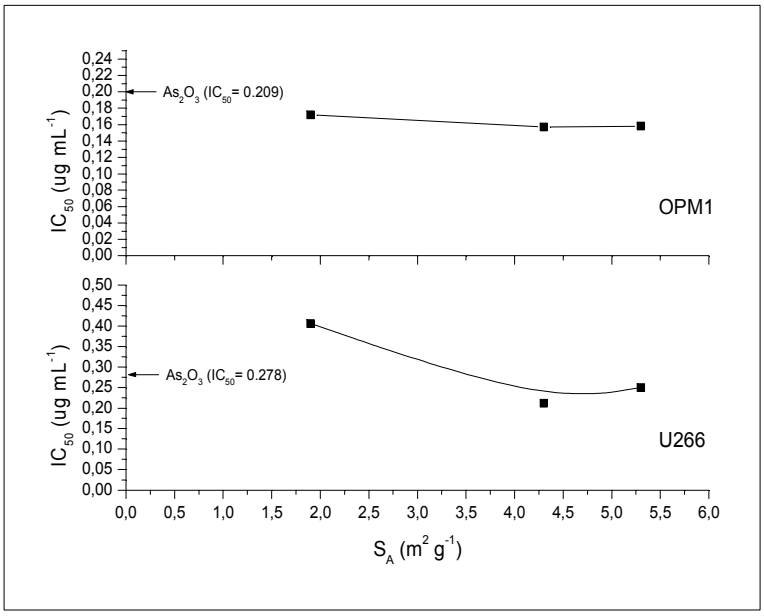

Fig. 4 IC_{50} values of multiple myeloma cancer cell lines vs. specific surface area of arsenic suphide nanoparticles

Dissolution in simulated gastric fluid. Because realgar nanoparticles are designed to disperse in the stomach's contents, dissolution in simulated gastric fluid (SGF) should provide an initial estimate of the dissolution rate enhancement [25]. Here, bioaccessibility, which is defined as the fraction of As that is soluble in the stomach environment and is available for uptake into the blood system, plays an important role. The results are given in Fig. 5. Arsenic concentration, in solution, increases with dissolution time; also, a dependence on the milling time is well-documented. In the literature [26-27], the bioaccessibility of arsenic sulphide was investigated, revealing that a maximum of 0.6 % As was solubilised by the simulated gastric fluid. In our case, the value 0.93 % As was obtained after dissolution for 30 min. This amount is available for absorption into the bloodstream. Generally, the obtained solubilisation is low, but there are potential methods for increasing it, e.g., by modifying SGF with the addition of pepsine, by modifying the pH values, or by optimising the milling process.

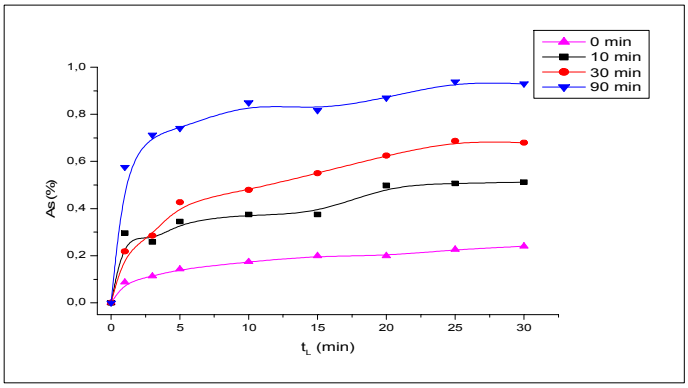

Fig. 5 Dissolution of As from arsenic suphide in simulated gastric fluid (SGF) vs. dissolution time, t_L

Conclusions

Changes in surface area, nanoparticle distribution and Raman scattering of realgar As_4S_4 nanoparticles were detected as consequences of high-energy wet milling. The treatment of two cancer cell lines, with the realgar nanoparticles, resulted in the decrease of cell viability. Dissolution in simulated gastric fluid shows a possible direction for future activities in cancer treatment, namely, the use of realgar nanoparticles in oral dosing as an alternative to intravenous administration of arsenic oxide.

Acknowledgements

This work was supported by VEGA grant 2/0009/11 and APVV grants LPP-0107-09 and APVV-0189-10.

References

[1] P. Bonazzi and L. Bindi: Z. Kristallogr. Vol. 223 (2008), p. 132.

[2] M. Popescu, J. Non-Cryst. Solids 352 (2006), p. 887.

[3] P.J. Dilda and P.J. Hogg: Can. Treat. Rev. 33 (2007), p. 542.

[4] J. Liu, Y. Lu, Q. Wu, G.A. Goyer and M.P. Waalkes: J. Pharm. Exper. Therap. Vol. 326 (2008), p. 363.

[5] P. Baláž: *Mechanochemistry in Nanoscience and Materials Engineering* (Springer, Germany 2008).

[6] E. Merisko-Liversidge, G.G. Liversidge and E.R. Cooper: Europ. J. Pharm. Sci. Vol. 18 (2003), p. 113.

[7] P. Baláž, M. Fabián, M. Pastorek, D. Cholujová and J. Sedlák: Mat. Lett. Vol. 63 (2009), p. 1542.

[8] E. Gaffet, F. Bernard, J.C. Niepce, F. Charlat, Ch. Gras, G. Le Caër, J.L. Guichard, P. Delcroix, A. Mocellin, O. Tillement: J. Mater. Chem. 9 (1999), p. 305.

[9] C. Suryanarayana: Progr. Mater. Sci. 46 (2001), p. 1.

[10] L. Takacs: Progr. Mater. Sci. 47 (2002), p. 355.

[11] F. Miani, F. Maurigh, in: *Dekker Encyklopedia of Nanoscience and Nanotechnology,* edited by J.A. Schwarz, C.J. Contescu and K. Putyera, Marcel Dekker, New York (2004), p. 1787.

[12] T.P. Shakhtshneider: Sol. St. Ionics 101-103 (1997), p. 851.

[13] V.V. Boldyrev: J. Mater. Sci. 39 (2004), p. 5117.

[14] J.Z. Wu and P.C. Ho: Europ. J. Pharm. Sci. 29 (2006), p. 35.

[15] D. Hörter, J.B. Dressman: Adv. Dr. Del. Rev. 46 (2001), p. 75.

[16] T. Mosmann: J. Immun. Meth. 65 (1983), p. 55.

[17] D. Bartkowiak, S. Hogner, H. Baust, W. Nothdurft, E.M. Rottinger: Cytom. 37 (1999), p. 191.

[18] A.Z. Juhász, L. Opoczky: *Mechanical Activation of Minerals by Grinding: Pulverizing and Morphology of Particles* (Ellis Horwood, Chichester 1990).

[19] R. Forneris: Am. Mineral. 54 (1969), p. 1062.

[20] P. Bonazzi, S. Menchetti, G. Pratesi, M. Muniz-Miranda, G. Sbrana: Am. Mineral. 81 (1996), p. 874.

[21] P. Baláž, W.S. Choi and E. Dutková: J. Phys. Chem. Sol. Vol. 68 (2007), p. 1178.

[22] P. Naumov, P. Makreski, G. Jovanovski: Inorg. Chem. 46 (2007), p. 10624.

[23] P. Naumov, P. Makreski, G. Petruševski, T. Runčevski, G. Jovanovski: J. Am. Chem. Soc. 132 (2010), p. 11398.

[24] Z.Y. Wang: Can. Chem. Pharm. 48 (Suppl. 1) (2001), p. 72.

[25] F. Kessisoglou, S. Pannai, Y. Wu: Adv. Dr. Del. Sys. 59 (2007), p. 631.

[26] S.Y. Kwan, S.K. Tsui, T.O. Man: Anal. Lett. 34 (2001), p. 1431.

[27] X.H. Wu, D.H. Sun: Anal. Chim. Acta 453 (2002), p. 311.

Journal of Nano Research Vols. 18-19
10.4028/www.scientific.net/JNanoR.18-19

Arsenic Sulphide As₄S₄ Nanoparticles: Physico-Chemical Properties and Anticancer Effects

10.4028/www.scientific.net/JNanoR.18-19.149